Journal of Advanced Ceramics
2012, 1(1): 24-37
DOI: 10.1007/s40145-012-0003-3 ISSN 2226-4108

Review

(K, Na)NbO_3-based lead-free piezoceramics: Phase transition, sintering and property enhancement

Ke WANG, Jing-Feng LI *

State Key Laboratory of New Ceramic and Fine Processing, Department of Materials Science and Engineering, Tsinghua University, Beijing 100084, China

Received February 16, 2012; Accepted March 1, 2012

Abstract: Most widely used piezoelectric ceramics are based on $Pb(Zr,Ti)O_3$ (PZT) composition which has adverse environmental and health effects due to its high lead content. Environmental and safety concerns with respect to the utilization, recycling, and disposal of lead-based piezoelectric ceramics have induced a new surge in developing lead-free piezoelectric ceramics. Among all the lead-free ceramics, $(K,Na)NbO_3$ (KNN) has drawn increasing attention because of its well-balanced piezoelectric properties and better environmental compatibility. On basis of the author's work, this review summarizes the progress that has been made in recent years on development of KNN-based piezoelectric ceramics, including crystallographic structure and phase transition analysis, pressurized solid-state sintering as well as liquid-phase-assisted sintering process, and poling treatment for property enhancement. All in all, KNN is a promising lead-free system, but more research is still required both from academic and industrial interests.

Key words: electrical properties; ferroelectric properties; piezoelectric properties; perovskites; niobates; lead-free

1 Introduction

In the 1880s, Pierre and Jacque Curie discovered that some crystalline materials, when compressed, produce a voltage proportional to the applied pressure. This characteristic is called piezoelectricity [1]. Although piezoelectricity is found in several types of natural materials, most modern devices use polycrystalline ceramics. Piezoelectric ceramics, which play an important role as functional electronic materials, have been widely used in various applications such as sensors, actuators transducers and so on. For decades, lead zirconate titanate ($Pb(Zr_{1-x}Ti_x)O_3$ or PZT) ceramics has been market-dominating due to its excellent properties. Generally, the commonly used compositions are along a morphotropic phase boundary (MPB) around $x = 0.48$ separating tetragonal and rhombohedral phases, where dielectric, piezoelectric, and electromechanical coupling properties are optimized. The origin of the enhanced properties of PZT at the morphotropic phase boundary has been investigated in detail by many authors and is still a topic of intense interest. Several mechanisms have been invoked to explain the enhanced piezoelectric properties of PZT at MPB. However,

* Corresponding author.
E-mail: jingfeng@mail.tsinghua.edu.cn

there is still no consensus in the literature on this issue. A widely accepted perspective believes that the increased properties are due to enhanced polarizability arising from the equivalent energy state between tetragonal and rhombohedral phases, which underlies optimal domain rotation during the poling process.

However, the large amount of lead contained in PZT materials has drawn much attention during the past decade, due to the environmental concern as well as government regulations against hazardous substances. In 2006, the European Union has already adopted the well-known directives Waste Electrical and Electronic Equipment (WEEE) and Restriction of the use of certain Hazardous Substances in electrical and electronic equipment (RoHS), with the purpose of protecting human health as well as environment by exclusion or substitution of hazardous substances used in electrical and electronic devices [2,3]. Similar regulations are also planned or established in North America, Japan, Korea and China. Lead ranks foremost among the hazardous substances list due to its notoriety, with maximum allowed concentration of mere 0.1 wt%. However, PZT, which contains more than 60 wt% lead oxides, is still allowed to be used in piezoelectric devices all over the world up to now, since no alternative lead-free counterparts is available. Therefore, tremendous efforts have been devoted to the development of competitive lead-free counterparts, such as $BaTiO_3$, $Bi_{1/2}Na_{1/2}TiO_3$-based perovskites, bismuth layer-structured ferroelectrics (BLSF), and (K, Na)NbO_3 (KNN)-based perovskites, and so on. At the moment, great embarrassment has been encountered in search for one single qualified lead-free system substituting PZT, which is so versatile in properties by utilization of various doping elements that it can fit almost all purposes. Therefore, it is reasonable to penetrate deeply into these various lead-free systems, and take advantage of them in distinct circumstances.

Among all the lead-free candidates, alkali niobate ceramics based on KNN have drawn much attention since Saito *et al*. made the breakthrough in Li, Ta, and Sb-modified KNN ceramics with textured structure [4]. Despite pure KNN ceramics is normally considered with a piezoelectric constant d_{33} as low as around 80 pC/N, the value reported by Saito *et al*. reached amazingly up to 416 pC/N, comparable to that of soft PZT ceramics. At first, it is believed that dopants like Li, Ta and Sb could consist in the constitution of MPB in KNN-based ceramics, which mimics that in PZT ceramics and eventually results in the property enhancement. Thus, all kinds of dopants are exploited with special emphasis on the improvement of piezoelectric constant d_{33}, which is usually measured using the convenient quasi-static method (Berlincourt-meter method) and taken as the small signal d_{33}. Generally, the most effective approach for property enhancement of KNN-based ceramics is to form solid solutions with other species, such as $LiNbO_3$ [5-12], $LiTaO_3$ [7,13-20], $LiSbO_3$ [21-23], $BaTiO_3$ [24,25], $CaTiO_3$ [26-30], $(Bi_{0.5}Na_{0.5})TiO_3$ [31-35], or a combination of multiple additives [30,36-51], and typical d_{33} values obtained are among 200~300 pC/N. Later on, it is proposed that the underlying mechanism for property enhancement of KNN-based ceramics by means of above-mentioned manners is not classical MPB but PPT, which is the abbreviation of polymorphism phase transition and exists in many materials such as $BaTiO_3$ [15]. The key point of PPT theory claims that property enhancement in KNN-based ceramics is due to tetragonal-orthorhombic polymorphism phase transition point ($T_{O\text{-}T}$) shifting downwards from around 200 ℃ to room temperature. However, MPB is actually more favorable over PPT since PPT has a problem of temperature instability [27,46]. As a result, the development of KNN-based ceramics is retarded for the time being, the situation of which has been encountered before by many great scientific innovations. Fortunately, several tentative ideas have already been brought out to further exploiting the potential of KNN-based materials as next generation lead-free piezoceramics [52-54].

Technically, it seems that the situation in KNN-based system is more complicated than that of traditional PZT series, which has invoked so many interesting scientific discussions. The authors have been working on KNN-based ceramics for almost 10 years, and would like to share these little tiny experiences with those who have already working on or will jump into this field. Certainly, there are already excellent reviews with regard to lead-free piezoceramics [55-60], but none of them is dedicated to KNN-based ceramics. The present review covers topics over a broad range, including crystallographic structure, sintering techniques and poling tricks. Nevertheless, up to now the perception of KNN-based materials is still not in-depth, thus divergence on these issues may be found in literature.

2 Polymorphism and Property Enhancement

KNN ceramics were investigated intensively several decades ago both in material properties and structures [61,62], as it was found as a piezoelectric material in as early as 1950s [63]. It is well known that the most interesting compositions are located with K/Na ratio approximately equal to 1:1 [63-65], and the KNN ceramics mentioned hereafter refer to these compositions if no specific explanations provided. KNN ceramics have an orthorhombic structure with space group Amm2 at room temperature; however, it is a little complicated because it holds an orthorhombic structure while the perovskite type ABO_3 subcell possesses monoclinic symmetry [61]. Furthermore, there is no standard JAPDS-ICDD files for exact $K_{0.5}Na_{0.5}NbO_3$ even up to now. As a result, crystallographic indexing is inconsistent in literature, especially for researchers mainly focusing on materials properties. So what really happens to the structure of KNN-based ceramics is not clear enough. Furthermore, the enhanced piezoelectric properties in the modified KNN were firstly attributed to the formation of the MPB similar to that observed in the PZT system [5,11,36,45], which was later on pointed out to be a different effect namely polymorphic phase transition (PPT) [15,22]. In any case, phase structure investigations in KNN-based ceramics are of paramount importance for obtaining excellent properties.

Generally, pure KNN ceramics have the following polymorphisms, low temperature (<123 ℃) rhombohedral (R) phase, room temperature orthorhombic (O) phase, high temperature tetragonal (T, 200~410 ℃) and cubic (C, >410 ℃) phases [66]. Also, these phase transition temperatures can be tuned by introduction of dopants, such as Li, Ta, Sb, etc. In order to elucidate the crystalline structure of KNN and investigate the influence of dopants on the phase evolution as well as properties enhancement, $(1-x)(K_{0.5}Na_{0.5})NbO_3$-$xLiNbO_3$ ceramics were taken as an example in the following context to correlate material structures with piezoelectric properties [67]. Hence, a better understanding of phase structure and its relation with properties in KNN-based ceramics may be attained, which could possibly benefit researchers for properties enhancement.

The structure illustration for room temperature KNN is shown in Fig. 1. Although the structure of KNN at room temperature is orthorhombic, the perovskite type ABO_3 subcell, as shown in Fig. 1a,

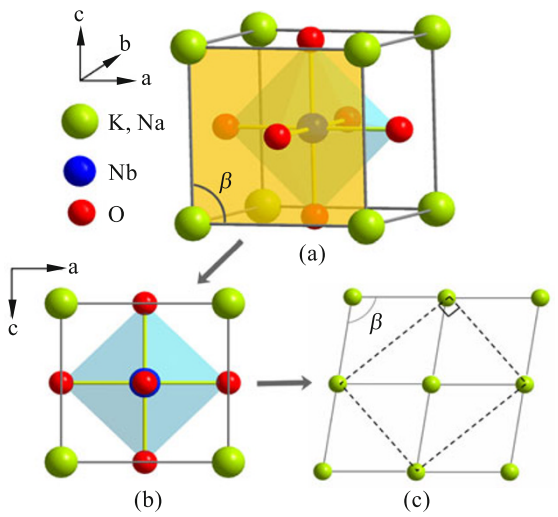

Fig. 1 The structure illustration for KNN of orthorhombic structure at room temperature (a) the perovskite type ABO_3 subcell; (b) the projection of the subcell along *b* axis; (c) four adjacent subcell projections in an exaggerated manner to show the geometrical relationship, while omitting Nb and O atoms. (Reprinted with permission from Ref. [67]. © 2007, American Institute of Physics)

possesses monoclinic symmetry, with lattice parameters $a_m = c_m > b_m$ while b_m axis is perpendicular to $a_m c_m$ plane and angle β a little more than 90°. For the composition $(K_{0.5}Na_{0.5})NbO_3$, which is believed to lie along the orthorhombic-orthorhombic MPB and possess the best performance in $KNbO_3$-$NaNbO_3$ system, no superlattice reflections were found in previous XRD measurements [61], and thus no corner-linked O octahedra tilting should be taken into account [68]. Projection view of the subcell along b_m axis is shown in Fig. 1b. Since angle β is very close to 90°, it looks like that a_m axis is also perpendicular to c_m axis. Therefore, in order to show the geometrical relationship more clearly, we could exaggerate angle β much more than 90°, and draw the projection of four adjacent perovskite subcells together, but omit Nb and O atoms, as shown in Fig. 1c. As a_m axis equals c_m axis in length, the diagonals linked by dashed lines in Fig. 1c form a rectangle, which is the projection of unit cell of KNN along b_m axis. Hence it could be easily understood that the perovskite type subcell of KNN is monoclinic while its unit cell has orthorhombic symmetry at room temperature. Furthermore, when temperature increases above 200 ℃, a phase transition from orthorhombic to tetragonal occurs in KNN [69], which is similar to that of $KNbO_3$, with space group

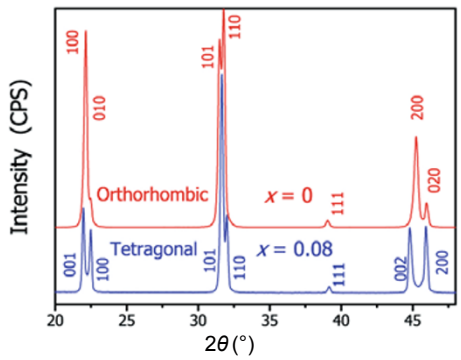

Fig. 2 The X-ray diffraction patterns of $(1\text{-}x)(K_{0.5}Na_{0.5})NbO_3\text{-}xLiNbO_3$ ceramics

changing from Amm2 to P4mm [70]. It is considered that dopants substitution, such as Li, in KNN would cause similar phase transition at room temperature. So in the tetragonal phase of Li-modified KNN, the perovskite type ABO_3 subcell is the unit cell itself, with lattice parameters $c_t > a_t = b_t$ and all three axes perpendicular with each other.

The above mentioned distinction between orthorhombic and tetragonal phases in KNN-based ceramics could be characterized by X-ray diffraction (XRD). The XRD patterns of $(1\text{-}x)(K_{0.5}Na_{0.5})NbO_3\text{-}xLiNbO_3$ ceramics are shown in Fig. 2, and the crystallographic indexing is according to the perovskite type ABO_3 subcell, both for orthorhombic structure when $x = 0$ and tetragonal structure when $x = 0.08$, respectively. It is certain that the structure variation is due to the large distortion caused by doping Li element. The difference of peak profiles around 45° in X-ray diffraction pattern is usually used as an evidence for the phase transition in literature, though why these peaks would change in such a manner, or what really happens to the structures is hardly mentioned. The phase transition of $(1\text{-}x)(K_{0.5}Na_{0.5})NbO_3\text{-}xLiNbO_3$ ceramics could be deduced from profiles of the $N = 12$ ({hkl} = {222}) and $N = 16$ ({hkl} = {400}) line groups in XRD patterns, as shown in Fig. 3. The splitting of the $N = 12$ line group, as shown in Fig. 3a, indicates the existence of angle β in the monoclinic perovskite subcell. The two peaks around 84° in the XRD pattern when $x = 0$ tend to merge into one single peak with increasing Li amount, responding to the decrease in angle β. On the other hand, the $N = 16$ line group, as shown in Fig. 3b, shows the change of the three axes length in the subcell. It is obvious that in the orthorhombic phase when x=0, the intensity of the peak near 100° is larger than that of the one near 103°, because $a_m = c_m > b_m$; while in the tetragonal phase the opposite situation occurs due to $c_t > a_t = b_t$. Therefore, when $x = 0.06$, the two contiguous peaks around 84° and the widely broadening peak around 99° obviously represent an intermediate state, showing the two phases co-existence condition. In addition, Raman spectroscopy is also an useful and convenient technique for phase identification of KNN-based piezoceramics [10,15,65,66,71-73].

As for property enhancement, shifting downward of tetragonal-orthorhombic transition ($T_{O\text{-}T}$) point to room temperature by doping or forming solid solutions in KNN with other species do increase piezoelectric constant d_{33} to a level of 200~300 pC/N, while pure KNN ceramics suffering a relative low d_{33} around 80 pC/N. The fatal drawback is temperature instability [27, 46], which is absent in PZT systems due to existence of genuine MPB other than PPT. Apart from concerns about temperature instability of properties, it is noted that for identical or similar compositions of KNN-based ceramics, obtained properties could vary a lot among different research groups, which is possibly due to the exact location of $T_{O\text{-}T}$. Recently, it is reported

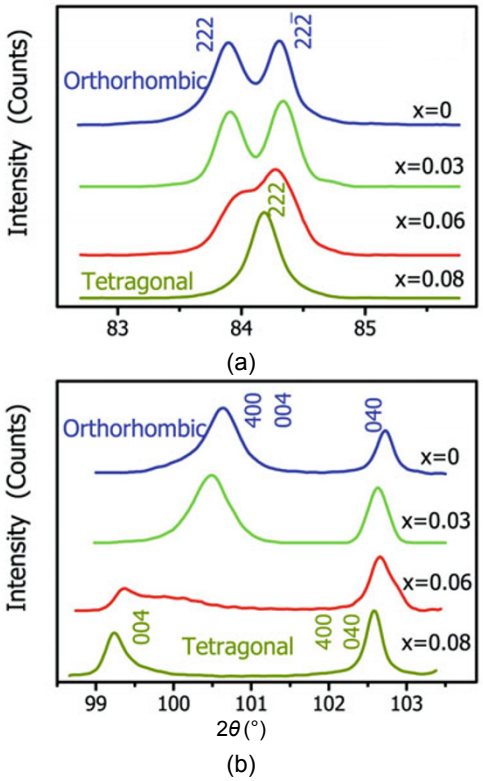

Fig. 3 The X-ray diffraction patterns of $N = 12$ and $N = 16$ groups in $(1\text{-}x)(K_{0.5}Na_{0.5})NbO_3\text{-}xLiNbO_3$ ceramics

that the $T_{O\text{-}T}$ could even be influenced as much as tens of degrees due to intergranular stress [73]. Besides, property enhancement in KNN-based ceramics appears to come a halt, which is actually the bottleneck effect of PPT. As a result, designing a PZT-like MPB in KNN systems seems more practical. The success of constructing a tricritical triple point in $BaTiO_3$ system [74,75], as well as similar attempt in KNN-based ceramics [54], could probably offer fresh and innovative ideas for the future.

3 Sintering techniques

3.1 Spark plasma sintering (SPS)

Sintering has been among the most active topics for KNN-based materials ever since it was first discovered half a century ago [63,76,77], due to intrinsic volatility of alkaline species. Thus, normal sintering (in contrast to pressure-assisted sintering like hot-pressing or spark plasma sintering) of KNN-based materials often has a chance to encounter with low density and poor microstructure, which definitely degrades piezoelectric performance. Due to the poor sinterability and high volatility of KNN, pressure-assisted sintering techniques have been utilized for pursuing high density. Jaeger and Egerton [76] firstly fabricated highly dense KNN ceramics using hot pressing and reported that the hot-pressed samples possessed high piezoelectric constants and Curie temperature. Recently, spark plasma sintering (SPS) has been increasingly used instead of conventional hot pressing because of its advantages of a rapid heating rate and short soaking time. Our group has done a series of systematic studies on SPS of KNN-based ceramics, with special emphasis on property enhancement [78-83].

Sodium potassium niobate ceramics with the nominal composition of $K_{0.5}Na_{0.5}NbO_3$ were fabricated successfully using SPS at a low temperature of 920 ℃. By post-annealing treatment in air, the SPS-processed $K_{0.5}Na_{0.5}NbO_3$ ceramic samples showed typical ferroelectric and piezoelectric characteristics. The room temperature dielectric constants at 1, 10, 100, and 1000 kHz are 606, 584, 559, and 571, respectively, with dielectric loss values being in the range of 0.026 ~ 0.044. Although the grain sizes are small comparing with normally sintered samples (see Fig. 4), being on the order of 200 ~500 nm, the resultant $K_{0.5}Na_{0.5}NbO_3$ ceramics show a considerably high d_{33} of 148 pC/N. It is suggested that the enhancement is the result of extrinsic contributions to the polarizability associated with submicron grain sizes [55]. Similar result was also found in fine-grained $BaTiO_3$ ceramics [84].

In addition to pure KNN samples, Li and Ta co-doped KNN ceramics were also investigated by SPS method [81]. Dense and fine-grained $(Na_{0.535}K_{0.485})_{1-x}$-$Li_x(Nb_{0.8}Ta_{0.2})O_3$ (x=0.02~0.07) (abbreviated as NKL_xNT) lead-free piezoceramics were fabricated by SPS at around 900 ℃, followed by post-annealing in air. All the NKL_xNT ceramics showed single perovskite structures with a phase transition from an orthorhombic symmetry to a tetragonal one across a composition region of x=0.04~0.05. The sample with a composition of x=0.05 had the maximum values of piezoelectric coefficient (d_{33}=243 pC/N) and planar electromechanical coupling coefficient (k_p=46.1%), and other good properties such as Q_m = 85, ε_r = 1240, and tan δ = 0.023. Because of the enhanced densification and refined microstructure, the SPS-processed NKL_xNT ceramics also had better fracture strength

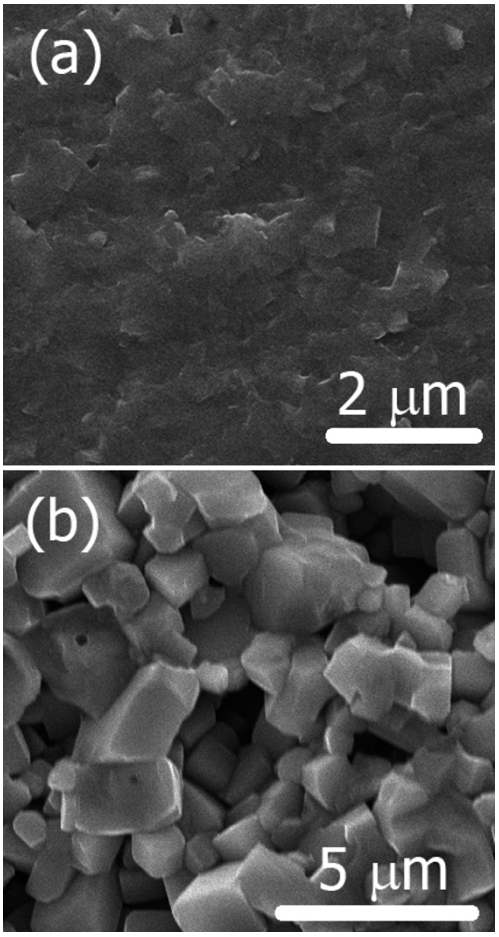

Fig. 4 SEM micrographs of (a) SPS and (b) normally sintered $(K_{0.5}Na_{0.5})NbO_3$ ceramics

than that prepared by normal sintering.

3.2 Normal solid state sintering

Normal sintering is cost-effective and simple, which is of great attraction for mass production. So, investigation on normal sintering of KNN never ceases. It was found that in normal sintering of KNN-based ceramics, density increased greatly within a narrow temperature range but turned to decrease when the sintering temperature slightly exceeded the optimal one. Piezoelectric properties also showed similar relationship between the density and sintering temperature, but the highest piezoelectric strain coefficients were obtained at the temperatures lower than that for the highest density [85,86].

Figure 5 shows the change in the sintered densities of the KNN, Li-KNN (LKNN) and Li/Ta-KNN (LKNNT) samples as a function of sintering temperature. It was found that the change in density was very sensitive to the sintering temperature. Even though the sintering temperature was changed within a narrow range, the resultant density changed significantly for all the compositions. The density increased rapidly and then decreased slowly after reaching a maximum. Ta doping apparently shifted the maximum sintering point to higher temperature, whereas the densification behavior was almost the same both for the samples without and with Li doping. The highest density values obtained for the three compositions exceeded 95% of their theoretical densities. Fig. 5 also shows the changes in piezoelectric coefficient d_{33} of the three compositions as a function of sintering temperature. It is interesting that similar tendencies were obtained for the relationship between d_{33} and sintering temperature as the case of sintered density. All the three compositions showed their peak d_{33} values at their corresponding sintering temperatures. However, it must be noted that the temperature where the maximum d_{33} value was obtained differed from the point where the peak density was achieved. For example, the highest density was obtained at 1120 ℃ for the LKNNT composition, whereas d_{33} of the resultant ceramics sample decreased apparently from the peak point if sintered at 1120 ℃; the highest d_{33} value was obtained at the temperature which is about 20~30 ℃ lower than that where the highest density can be reached. In other words, the d_{33} values dropped apparently when sintered at the temperatures exceeding the points that correspond to the peak density. On the other hand, the d_{33} values of the samples were relatively high, in spite of their low density when sintered at the temperatures below the point corresponding to the peak density.

The main question about the above results is why the optimal sintering temperature for the electrical properties differed from that for the density? As shown above, the piezoelectric and dielectric properties changed with a similar tendency as the relationship between density and sintering temperature. However, the sintering temperatures where the highest d_{33} values were obtained, were not consistent with that where the highest density was reached. To answer this question, we must take into account the volatilization of alkali components during the sintering, which occurred during the sintering of KNN-based ceramics and caused the composition deviation from the starting one. The volatilization may be accelerated when the liquid phase appears, although which also enhances the densification at the same time. Our study by inductively coupled plasma (ICP) analysis confirmed the serious volatilization above 1000 ℃, as shown in Fig. 6. Considering that the electric properties are sensitive to the composition change [6,79,87,88], and

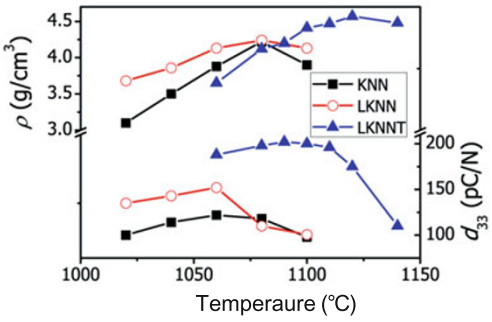

Fig. 5 Density and piezoelectric coefficient d_{33} of KNN, LKNN and LKNNT samples as a function of sintering temperature

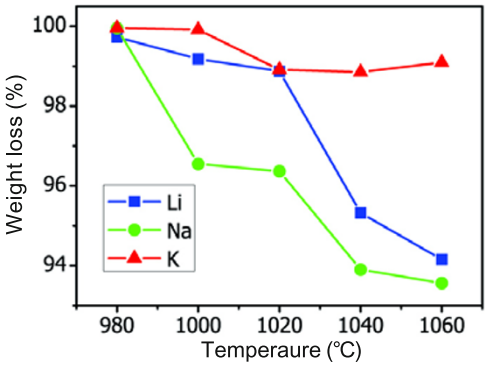

Fig. 6 Weight loss of alkaline elements in KNN-based ceramics as a function of sintering temperature

that the sample sintered to the highest density may not have the optimal composition, it is easy to understand why the highest piezoelectric and dielectric properties were obtained at somewhat lower sintering temperature than that for density. In addition, grain coarsening or abnormal grain growth occurred when the sintering temperature exceeded the peak point for the density, which may also not be favorable for the optimization of electrical properties [89].

3.3 Low-temperature liquid-phase sintering

Technically, the low-temperature sintering mentioned here is still in the discussion range of normal sintering. However, the densification mechanism during sintering is different due to emergency of a liquid phase, and the low-temperature sintering is greatly effective for property enhancement. As a result, we take out this topic as a separate section. As explained in the previous section, the properties of KNN-based ceramics are extremely sensitive to the processing conditions, especially the sintering temperature. The sintering temperatures are usually very high as compared with the melting points in the phase diagram, easily causing severe volatilization of alkali elements (see Fig. 6), and resulting in a composition deviation and hence property degradation. For example, in our previous study on Li-doped KNN ceramics, the d_{33} value decreases from a peak (314 pC/N) to about 220 pC/N if sintered at a temperature just 20 ℃ higher than the optimized one (1060 ℃) for the KNN-ceramics containing 5.8 mol% $LiNbO_3$ [6]. Therefore, it is necessary to develop low-temperature sintering processes for KNN-based ceramics. Also, low-temperature sintering could satisfy the demand for co-firing KNN-based ceramics with metal electrodes for device applications. Recently, our study revealed that Li-modified KNN lead-free piezoceramics can be sintered at a temperature as low as 950 ℃, whose d_{33} value is up to 280 pC/N [12,90]. This result shows that low temperature sintering and high performance could be achieved together in high-performance $LiNbO_3$-KNN lead-free piezoceramics, which are of great potential for industrial applications. It is believed that the success of low-temperature sintering is related to the excess amount of Na_2O added intentionally.

The addition of excess amount of Na_2O could effectively reduce the sintering temperatures of Li-modified KNN ceramics. Figure 7 shows the shrinkage curve of $(1-x)(Na_{0.535}K_{0.48})NbO_3$-$xLiNbO_3$ at x = 0.08, which clearly demonstrates that the sample started to shrink at the temperature as low as 800 ℃, while the shrinkage rate had an abrupt change at 930 ℃. The nearly vertical shrinkage rate curve after 930 ℃ suggests an unusually fast densification process, which is due to the formation of liquid phase. Although Na_2O was added with excess amount, the effective sintering aid may be involved with other species. It was reported that A_2O (A = Li, Na, K) could all form eutectic phases with Nb_2O_5, for mole ratio A:Nb more than 1:1, with melting points around 800 ℃; while A_2CO_3 (A = Li, Na, K), some of which probably remained in the matrix after calcination at 750 ℃ since extra Na_2CO_3 was added initially, also has melting points lower than 950 ℃. Considering that Li^+, Na^+, and K^+ could all fill into the A site of perovskite subcell, the actual liquid phase may be eutectic phases formed between any of A_2O (A = Li, Na, K) and Nb_2O_5, or remnant carbonates A_2CO_3 (A = Li, Na, K). The inner figures in Fig. 7 shows the SEM micrographs of $(1-x)(Na_{0.535}K_{0.48})NbO_3$-$xLiNbO_3$ with x = 0.08 sintered at 900℃ and 950 ℃, respectively. The average grain size of the sample sintered at 900 ℃ is about 1-2 μm, and only a few of grains are adhered together with a low density of 3.95 g/cm^3. The loose microstructure indicates no appearance of liquid phase at 900 ℃. By contrast, when the sample was sintered at 950 ℃, the microstructure changed significantly, with some large quadrate grains of 20 to 40 μm and an enhanced density of 4.36 g/cm^3. Within a merely 50 ℃ difference in sintering temperatures, the grain size increased from 1~2 μm to several tens of microns, confirming the effectiveness of liquid phase sintering. It has been recognized that the driving force for sintering is the decrease of surface energy of whole system. As for this case of liquid phase sintering, three

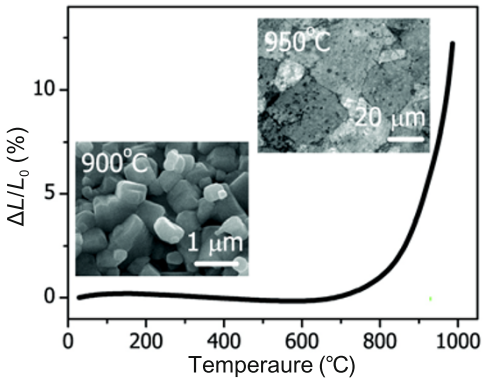

Fig. 7 Shrinkage curve and SEM micrographs of $0.92(Na_{0.535}K_{0.48})NbO_3$-$0.08LiNbO_3$

Table 1 Properties and phase structures of $0.92(Na_{0.535}K_{0.48})NbO_3$-$0.083LiNbO_3$ samples sintered at different temperatures

Temp. (℃)	850	900	930	950	970	1000	1050	1100
ρ (g/cm^3)	3.40	3.96	4.27	4.38	4.32	4.16	4.13	4.06
ρ, relative (%)	75.4	87.8	94.7	97.1	95.8	92.2	91.6	90.0
d_{33} (pC/N)	135	195	230	280	200	125	110	100
Phase structure*	O	O-T	O-T	O-T	O-T	T	T	-

* O is abbreviation for orthorhombic, and T is for tetragonal. "-" means ambiguous phase identification due to emergence of impurities

distinct stages have been classified [91]: (1) particle rearrangement, (2) solution-precipitation process, and (3) coalescence process. The morphology of the 950 ℃-sintered sample demonstrates that it was at the final stage of liquid phase sintering, with substantially dense micro- structure and large faceted grains exhibiting shape accommodation characteristic for maximum density.

Table 1 shows the sintered density and piezoelectric coefficient d_{33} as a function of sintering temperature for the sample of x=0.080. The density increases significantly as the sintering temperature is increased from 850 to 950 ℃, and reaches a peak, then decreases gradually with further increasing sintering temperature. The bulk density (about 4.38 g/cm^3) obtained at 950 ℃ is higher than 95% of the theoretical density. The densification behavior can be also confirmed by the microstructure observation. This result is surprising because low-temperature sintering was realized by simply adding excessive Na_2O, which is important for co-firing KNN-based multilayer with the Ag/Pd electrode. Although the low-temperature sintering mechanism is not yet clearly understood, liquid-phase sintering should be responsible for the densification. The grain growth behavior seems to be a clear indicator supporting our consideration about liquid-phase sintering, because the grain sizes increased exceptionally as the sintering temperature was raised from 900 to 950 ℃. The density decreases when sintered above 950 ℃ probably because the volatilization of alkali oxides is accelerated, which is not in favor of the formation of liquid phase. In fact, the weight loss at 950 ℃ and 1050 ℃ were 0.5% and 1.3%, respectively. In addition to the highest density, a peak d_{33} was obtained when sintered at 950 ℃ for the x=0.080 composition, also because it consisted of orthorhombic and tetragonal phases. It should be noted that for the same x=0.080 composition, the resultant phase structure also changed from orthorhombic to tetragonal with increasing sintering temperatures, as revealed in Table 1, which is the result of volatilization of alkaline species.

4 Poling tricks

It is known that poling is an important process to endow ferroelectric ceramics with macroscopic piezoelectric responses, by applying a high electric field up to several thousand voltages per millimeter. Inferior ferroelectric response is obtained by insufficient poling, which is caused by various factors such as defects. The effect of poling conditions on the dielectric and piezoelectric properties of KNN-based ceramics has been a subject of recent studies [92-97], most of which pointed out that poling temperature is of significant importance for property enhancement. Nevertheless, poling process could also be utilized to manipulate interior dipole movement, which might be tuned to favorable piezoelectric performance [52,53].

For a compositionally optimized Li-doped composition, its piezoelectric coefficient d_{33} can be increased up to 324 pC/N even from a considerably high value (190 pC/N) by means of re-poling treatment after room temperature aging; such a high d_{33} value is only reachable in literature for KNN ceramics with complicated modifications using Ta and Sb dopants [46,98,99]. Table 2 shows the piezoelectric coefficient d_{33} as well as tetragonal-orthorhombic phase transition temperature ($T_{O\text{-}T}$) of Li-doped KNN ceramics with respect to Li content, after both the first and second poling, respectively. Even though the sintering temperature was as low as 950 ℃, a high piezoelectric constants d_{33} up to 280 pC/N was obtained at an optimal composition of x=0.083 after the first poling. The basic mechanism for piezoelectric property enhancement in the present study was generally considered due to two-phase coexistence [15], which was denoted by a downward of $T_{O\text{-}T}$ to around room

Table 2 Piezoelectric properties and tetragonal-orthorhombic phase transition temperature ($T_{O\text{-}T}$) of $(1\text{-}x)(K_{0.5}Na_{0.5})NbO_3\text{-}x LiNbO_3$ after both the first and second poling

x	5.8	6.5	7	7.5	7.8	8	8.3	8.5
1st poled d_{33} (pC/N)	125	130	145	170	185	190	280	180
2nd poled d_{33} (pC/N)	128	135	170	230	260	324	255	145
$T_{O\text{-}T}$ (℃)	155	115	105	90	68	60	43	27

temperature, as also listed in Table 2. In spite of the considerably high piezoelectric performance of Li-doped KNN ceramics after the first poling treatment, the improvement of d_{33} after the second poling process is much more attractive, with a peak d_{33} of 324 pC/N at x=0.080, as shown in Table 2. It should be noted that more and more increment was made in d_{33} after the second poling with increasing Li content, with a maximum of 134 pC/N (from 190 to 324 pC/N) at x = 0.080. The maximum increment rate was amazingly more than 70%, even though no special treatment was given to the samples but just re-poling after aging for two months. However, the sample with an excellent d_{33} = 280 pC/N at x = 0.083 after the first poling showed no increase in d_{33} after re-poling two months later, but its d_{33} turned to decrease by 25 pC/N. It seems that aging and re-poling could not increase d_{33} for the $x \geqslant 0.083$ samples. In view of the $T_{O\text{-}T}$ and XRD measurements, it could be easily concluded that samples with coexisting phases at room temperature are favorable for the aging and re-poling induced enhancement of piezoelectricity, while those dominated by orthorhombic (with $T_{O\text{-}T}$ more than 120 ℃) or tetragonal phases are neither sensitive nor profited. For the ferroelectric properties, it was found that the second poling resulted in an increasing P_r from 6.78 to 14.46 μC/cm^2, and a reduced E_c from 22.52 to 17.58 kV/cm, respectively. The striking increase of d_{33} in the present study was due to large improvement of P_r [100].

As mentioned above, the increase of d_{33} was due to large improvement of P_r, which was accomplished by domain switching. Domain switching does not change the crystalline structure of the ceramics, but do make striking influences on macroscopic orientations of local atoms arrangement. XRD technique can provide accurate information concerning these variations by relative peaks intensity change, then domain evolution processes can be deduced. Figure 8 shows the XRD patterns of (222) and (004) lattice plane series for the x=0.080 sample, which were taken both before and after the first poling, as well as after the second poling, respectively. The peak indexing is adopted for a tetragonal phase. These high-angle X-ray diffractions offer phase information more precisely than the low-angle ones usually employed in literatures [67].

As shown in Fig. 8, for the as-sintered sample, higher intensity of the (400)/(040) peak over (004) peak is a clear symbol for the tetragonal phase since $c > a = b$; however, slight split of the (222) peak, and over-lifted kα2 line of (004) peak indicate the presence of the orthorhombic phase ($a = c > b$ with $90° < \beta < 91°$). After the first poling treatment, intensity contrast between (400)/(040) peak and (004) peak reverses, which is easily understood for the tetragonal phase due to an increase of c-domains. Besides, intensity increment of (004) peak after poling is also observed for the orthorhombic phase, despite the fact that <001> is not the spontaneous polarization direction. The increased intensity of (004) peak in orthorhombic phase can be easily deduced as a collateral consequence of domain rotation towards <110> directions. It should be emphasized that, significant

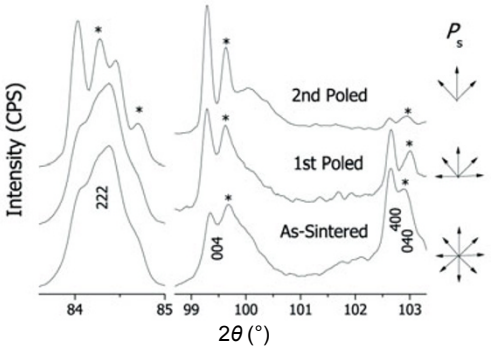

Fig. 8 Patterns of (222) and (004) lattice plane series for the sample $0.92(Na_{0.535}K_{0.48})NbO_3\text{-}0.08LiNbO_3$, both before and after the first poling, as well as after the second poling, respectively. The P_s evolution inside domains is listed aside, assuming that the electric field during poling is parallel to <001> direction

changes, represented by distinct split of (222) peak and almost disappearance of (400)/(040) peak, took place after the second poling. The deduced P_s evolution inside domains is listed aside in Fig. 8, assuming that the electric field during poling is parallel to the <001> direction. The P_s parallel to <100> and <010> directions after the first poling, switched to <001> direction after the second poling, which indicates that the non-switched 90° domains successfully rotated and kept constant by means of the aging and re-poling process. A mechanism corresponding to details of spontaneous polarization change in the domain level was proposed, concerning the combined effect of migration of oxygen vacancies, and interaction between defect dipoles and spontaneous polarization inside domains, which can be found elsewhere in detail [52].

It is widely accepted that poling of KNN-based ceramics is usually companied with problems, such as large leakage current, easy breakdown, etc.; however, the above results demonstrate that poling is also a chance which could be resorted for property enhancement. If poling condition could be optimized for a specific composition, very high d_{33} can be obtained without complicated doping compositions.

5 Summary

KNN-based ceramics has been investigated as a potential candidate for a new group of lead-free piezoelectric materials, and recent advances related to phase transitions, sintering techniques and property enhancement are discussed. Despite inferior piezoelectric response than PZT, KNN system is still favored by high Curie temperature, complete environment-friendliness, etc. The most urgent issue concerning development of KNN-based materials should be a breakthrough, both theoretically reasonable and experimentally testified, in property enhancement in the absence of PPT effect, such as real PZT-like MPB design. Then problems like temperature instability could be solved thoroughly. Also, secondary considerations, such as poling conditions, processing optimization, domain influences, etc., would be favored as well, due to request both practically and scientifically. Moreover, from the viewpoint of industrial application, d_{33} is not the only figure of merit. Actually, preliminary reports on piezoelectric devices utilizing KNN-based materials already exhibit promising results, including high-frequency ultrasonic transducers [101-103], surface acoustic wave (SAW) devices [29] and so on [104-107]. Although it is possible that KNN cannot carry out the historical assignment to substitute PZT everywhere, it must find suitable opportunities to fulfill itself eventually.

Acknowledgement

The authors appreciate the support by Tsinghua University Initiative Scientific Research Program and National Nature Science Foundation of China (Grant Nos. 50921061 and 51028202).

References

[1] Jaffe B, Cook WR, Jaffe H. Piezoelectric Ceramics. New York: Academic Press, 1971.
[2] Eu-Directive 2002/96/Ec: Waste electrical and electronic equipment (WEEE). *Off J Eur Union* 2003, **46**: 24-38.
[3] Eu-Directive 2002/95/Ec: Restriction of the use of certain hazardous substances in electrical and electronic equipment (RoHS). *Off J Eur Union* 2003, **46**: 19-23.
[4] Saito Y, Takao H, Tani T, *et al.* Lead-free piezoceramics. *Nature* 2004, **432**: 84-87.
[5] Guo YP, Kakimoto K, Ohsato H. Phase transitional behavior and piezoelectric properties of $(Na_{0.5}K_{0.5})NbO_3$-$LiNbO_3$ ceramics. *Appl Phys Lett* 2004, **85**: 4121-4123.
[6] Zhao P, Zhang BP, Li JF. High piezoelectric d_{33} coefficient in Li-modified lead-free $(Na,K)NbO_3$ ceramics sintered at optimal temperature. *Appl Phys Lett* 2007, **90**: 242909.
[7] Hollenstein E, Davis M, Damjanovic D, *et al.* Piezoelectric properties of Li- and Ta-modified $(K_{0.5}Na_{0.5})NbO_3$ ceramics. *Appl Phys Lett* 2005, **87**: 182905.
[8] Matsubara M, Yamaguchi T, Kikuta K, *et al.* Effect of Li substitution on the piezoelectric properties of potassium sodium niobate ceramics. *Jpn J Appl Phys* 2005, **44**: 6136-6142.
[9] Du HL, Tang FS, Liu DJ, *et al.* The microstructure and ferroelectric properties of $(K_{0.5}Na_{0.5})NbO_3$-

$LiNbO_3$ lead-free piezoelectric ceramics. *Mater Sci Eng B-Solid State Mater Adv Technol* 2007, **136**: 165-169.

[10] Klein N, Hollenstein E, Damjanovic D, *et al.* A study of the phase diagram of (K,Na,Li)NbO_3 determined by dielectric and piezoelectric measurements, and raman spectroscopy. *J Appl Phys* 2007, **102**: 014112.

[11] Song HC, Cho KH, Park HY, *et al.* Microstructure and piezoelectric properties of (1-*x*)($Na_{0.5}K_{0.5}$)NbO_3-*x*$LiNbO_3$ ceramics. *J Am Ceram Soc* 2007, **90**: 1812-1816.

[12] Wang K, Li J F, Liu N. Piezoelectric properties of low-temperature sintered Li-modified (Na, K)NbO_3 lead-free ceramics. *Appl Phys Lett* 2008, **93**: 092904.

[13] Guo YP, Kakimoto K, Ohsato H. ($Na_{0.5}K_{0.5}$)NbO_3-$LiTaO_3$ lead-free piezoelectric ceramics. *Mater Lett* 2005, **59**: 241-244.

[14] Zhao P, Zhang BP, Li JF. Enhancing piezoelectric d_{33} coefficient in Li/Ta-codoped lead-free (Na,K)NbO_3 ceramics by compensating Na and K at a fixed ratio. *Appl Phys Lett* 2007, **91**: 172901.

[15] Dai YJ, Zhang XW, Zhou GY. Phase transitional behavior in $K_{0.5}Na_{0.5}NbO_3$-$LiTaO_3$ ceramics. *Appl Phys Lett* 2007, **90**: 262903.

[16] Kim MS, Jeong SJ, Song JS. Microstructures and piezoelectric properties in the Li_2O-excess 0.95($Na_{0.5}K_{0.5}$)NbO_3-0.05$LiTaO_3$ cramics. *J Am Ceram Soc* 2007, **90**: 3338-3340.

[17] Lin D, Kwok KW, Chan HLW. Microstructure, phase transition, and electrical properties of ($K_{0.5}Na_{0.5}$)$_{1-x}$$Li_x$($Nb_{1-y}Ta_y$)$O_3$ lead-free piezoelectric ceramics. *J Appl Phys* 2007, **102**: 034102.

[18] Chang YF, Yang ZP, Ma DF, *et al.* Phase transitional behavior, microstructure, and electrical properties in Ta-modified [($K_{0.458}Na_{0.542}$)$_{0.96}Li_{0.04}$]NbO_3 lead-free piezoelectric ceramics. *J Appl Phys* 2008, **104**: 024109.

[19] Wu L, Zhang JL, Shao SF, *et al.* Phase coexistence and high piezoelectric properties in ($K_{0.40}Na_{0.60}$)$_{0.96}Li_{0.04}Nb_{0.80}Ta_{0.20}O_3$ ceramics. *J Phys D: Appl Phys* 2008, **41**: 035402.

[20] Zuo RZ, Ye C, Fang XS, *et al.* Processing and piezoelectric poperties of ($Na_{0.5}K_{0.5}$)$_{0.96}Li_{0.04}$($Ta_{0.1}Nb_{0.9}$)$_{1-x}Cu_xO_{3-3x/2}$ lead-free ceramics. *J Am Ceram Soc* 2008, **91**: 914-917.

[21] Zang GZ, Wang JF, Chen HC, *et al.* Perovskite ($Na_{0.5}K_{0.5}$)$_{1-x}$($LiSb$)$_x$$Nb_{1-x}O_3$ lead-free piezoceramics. *Appl Phys Lett* 2006, **88**: 212908.

[22] Zhang SJ, Xia R, Shrout TR, *et al.* Piezoelectric properties in provskite 0.948($K_{0.5}Na_{0.5}$)NbO_3-0.052$LiSbO_3$ lead-free ceramics. *J Appl Phys* 2006, **100**: 104108.

[23] Wu JG, Xiao DQ, Wang YY, *et al.* Effects of K content on the dielectric, piezoelectric, and ferroelectric properties of 0.95(K_xNa_{1-x})NbO_3-0.05$LiSbO_3$ lead-free ceramics. *J Appl Phys* 2008, **103**: 024102.

[24] Park HY, Ahn CW, Song HC, *et al.* Microstructure and piezoelectric poperties of 0.95($Na_{0.5}K_{0.5}$)NbO_3-0.05$BaTiO_3$ ceramics. *Appl Phys Lett* 2006, **89**: 062906.

[25] Lin D, Kwok KW, Chan HLW. Structure, dielectric, and piezoelectric properties of CuO-doped $K_{0.5}Na_{0.5}NbO_3$-$BaTiO_3$ lead-free ceramics. *J Appl Phys* 2007, **102**: 074113.

[26] Park HY, Cho KH, Paik DS, *et al.* Microstructure and piezoelectric properties of lead-free (1-*x*)($Na_{0.5}K_{0.5}$)NbO_3-*x*$CaTiO_3$ ceramics. *J Appl Phys* 2007, **102**: 124101.

[27] Zhang SJ, Xia R, Shrout TR. Modified ($K_{0.5}Na_{0.5}$)NbO_3 based lead-free piezoelectrics with broad temperature usage range. *Appl Phys Lett* 2007, **91**: 132913.

[28] Chang RC, Chu SY, Lin YF, *et al.* The effects of sintering temperature on the properties of ($Na_{0.5}K_{0.5}$)NbO_3-$CaTiO_3$ based lead-free ceramics. *Sensor Actuat A-Phys* 2007, **138**: 355-360.

[29] Chang RC, Chu SY, Lin YF, *et al.* An investigation of ($Na_{0.5}K_{0.5}$)NbO_3-$CaTiO_3$ based lead-free ceramics and surface acoustic wave devices. *J Eur Ceram Soc* 2007, **27**: 4453-4460.

[30] Wu JG, Xiao DQ, Wang YY, *et al.* Improved temperature stability of $CaTiO_3$-modified [($K_{0.5}Na_{0.5}$)$_{0.96}$]$Li_{0.04}$]($Nb_{0.91}Sb_{0.05}Ta_{0.04}$)$O_3$ lead-free piezoelectric ceramics. *J Appl Phys* 2008, **104**: 024102.

[31] Zuo RZ, Fang XS, Ye C. Phase structures and electrical properties of new lead-free ($Na_{0.5}K_{0.5}$)NbO_3-($Bi_{0.5}Na_{0.5}$)TiO_3 ceramics. *Appl Phys Lett* 2007, **90**: 092904.

[32] Zuo RZ, Fang XS, Ye C, *et al.* Phase transitional behavior and piezoelectric properties of lead-free ($Na_{0.5}K_{0.5}$)NbO_3-($Bi_{0.5}K_{0.5}$)TiO_3 ceramics. *J Am Ceram Soc* 2007, **90**: 2424-2428.

[33] Zuo RZ, Ye C. Structures and piezoelectric properties of ($NaKLi$)$_{1-x}$($BiNaBa$)$_x$$Nb_{1-x}Ti_xO_3$ lead-free ceramics. *Appl Phys Lett* 2007, **91**: 062916.

[34] Du HL, Zhou WC, Luo F, *et al.* Structure and electrical properties' investigation of ($K_{0.5}Na_{0.5}$)NbO_3-($Bi_{0.5}Na_{0.5}$)TiO_3 lead-free piezo electric ceramics. *J Phys D: Appl Phys* 2008, **41**: 085416.

[35] Du HL, Zhou WC, Luo F, *et al.* Polymorphic phase transition dependence of piezoelectric properties in

$(K_{0.5}Na_{0.5})NbO_3$-$(Bi_{0.5}K_{0.5})TiO_3$ lead-free ceramics. *J Phys D: Appl Phys* 2008, **41**: 115413.

[36] Chang YF, Yang ZP, Hou YT, *et al.* Effects of Li content on the phase structure and electrical properties of lead-free $(K_{0.46-x/2}Na_{0.54-x/2}Li_x)$-$(Nb_{0.76}Ta_{0.20}Sb_{0.04})O_3$ ceramics. *Appl Phys Lett* 2007, **90**: 232905.

[37] Chang YF, Yang ZP, Wei LL. Microstructure, density, and dielectric properties of lead-free $(K_{0.44}Na_{0.52}Li_{0.04})$ $(Nb_{0.96-x}Ta_xSb_{0.04})O_3$ piezoelectric ceramics. *J Am Ceram Soc* 2007, **90**: 1656-1658.

[38] Hagh NM, Jadidian B, Safari A. Property-processing relationship in lead-free $(K,Na,Li)NbO_3$ solid solution system. *J Electroceram* 2007, **18**: 339-346.

[39] Lin DM, Kwok KW, Chan HLW. Phase structures and electrical properties of $K_{0.5}Na_{0.5}(Nb_{0.925}Ta_{0.075})O_3$-$LiSbO_3$ lead-free piezoelectric ceramics. *J Phys D: Appl Phys* 2007, **40**: 6060-6065.

[40] Lin DM, Kwok KW, Chan HLW. Effects of BaO on the structure and electrical properties of $0.95K_{0.5}Na_{0.5}(Nb_{0.94}Sb_{0.06})O_3$-$0.05LiTaO_3$ lead-free ceramics. *J Phys D: Appl Phys* 2007, **40**: 6778-6783.

[41] Qi P, Wang JF, Ming BQ, *et al.* Phase transition and high piezoactivity of Sb doped $(Na_{0.53}K_{0.435}Li_{0.035})$ $Nb_{0.94}Ta_{0.06}O_3$ lead-free ceramics. *Chinese Phys Lett* 2007, **24**: 3535-3538.

[42] Rubio-Marcos F, Ochoa P, Fernandez JF. Sintering and properties of lead-free $(K,Na,Li)(Nb,Ta,Sb)O_3$ ceramics. *J Eur Ceram Soc* 2007, **27**: 4125-4129.

[43] Wu JG, Wang YY, Xiao DQ, *et al.* Effects of Ag content on the phase structure and piezoelectric properties of $(K_{0.44-x}Na_{0.52}Li_{0.04}Ag_x)$-$(Nb_{0.91}Ta_{0.05}Sb_{0.04})O_3$ lead-free ceramics. *Appl Phys Lett* 2007, **91**: 132914.

[44] Wu JG, Xiao DQ, Wang YY, *et al.* Effects of K/Na ratio on the phase structure and electrical properties of $(K_xNa_{0.96-x}Li_{0.04})(Nb_{0.91}Ta_{0.05}Sb_{0.04})O_3$ lead-free ceramics. *Appl Phys Lett* 2007, **91**: 252907.

[45] Yang ZP, Chang YF, Wei LL. Phase transitional behavior and electrical properties of lead-free $(K_{0.44}Na_{0.52}Li_{0.04})(Nb_{0.96-x}Ta_xSb_{0.04})O_3$ piezoelectric ceramics. *Appl Phys Lett* 2007, **90**: 042911.

[46] Akdogan EK, Kerman K, Abazari M, *et al.* Origin of high piezoelectric activity in ferroelectric $(K_{0.44}Na_{0.52}Li_{0.04})(Nb_{0.84}Ta_{0.1}Sb_{0.06})O_3$ ceramics. *Appl Phys Lett* 2008, **92**: 112908.

[47] Juan D, Wang JF, Zang GZ, *et al.* $(Na_{0.52}K_{0.44}Li_{0.04})Nb_{0.9-x}Sb_xTa_{0.1}O_3$ lead-free piezoelectric ceramics with high performance and high Curie temperature. *Chinese Phys Lett* 2008, **25**: 1446-1448.

[48] Lin DM, Kwok KW, Lam KH, *et al.* Phase structure and electrical properties of $K_{0.5}Na_{0.5}(Nb_{0.94}Sb_{0.06})O_3$-$LiTaO_3$ lead-free piezoelectric ceramics. *J Phys D: Appl Phys* 2008, **41**: 052002.

[49] Wu JG, Peng T, Wang YY, *et al.* Phase structure and electrical properties of $(K_{0.48}Na_{0.52})(Nb_{0.95}Ta_{0.05})O_3$-$LiSbO_3$ lead-free piezoelectric ceramics. *J Am Ceram Soc* 2008, **91**: 319-321.

[50] Zhao P, Zhang BP, Tu R, *et al.* High piezoelectric d_{33} coefficient in Li/Ta/Sb-codoped lead-free $(Na,K)NbO_3$ ceramics sintered at optimal temperature. *J Am Ceram Soc* 2008, **91**: 3078-3081.

[51] Zuo RZ, Xu ZK, Li LT. Dielectric and piezoelectric properties of Fe_2O_3-doped $(Na_{0.5}K_{0.5})_{0.96}Li_{0.04}Nb_{0.86}$-$Ta_{0.1}Sb_{0.04}O_3$ lead-free ceramics. *J Phys Chem Solids* 2008, **69**: 1728-1732.

[52] Wang K, Li JF. Domain engineering of lead-free Li-modified $(K,Na)NbO_3$ polycrystals with highly enhanced piezoelectricity. *Adv Funct Mater* 2010, **20**: 1924-1929.

[53] Wang K, Li JF, Zhou JJ. High normalized strain obtained in Li-modified $(K,Na)NbO_3$ lead-free piezoceramics. *Appl Phys Express* 2011, **4**: 061501.

[54] Zuo RZ, Fu J. Rhombohedral-tetragonal phase coexistence and piezoelectric properties of $(NaK)(NbSb)O_3$-$LiTaO_3$-$BaZrO_3$ lead-free ceramics. *J Am Ceram Soc* 2011, **94**: 1467-1470.

[55] Shrout TR, Zhang SJ. Lead-free piezoelectric ceramics: alternatives for PZT? *J Electroceram* 2007, **19**: 111-124.

[56] Zhang SJ, Xia R, Shrout TR. Lead-free piezoelectric ceramics vs. PZT? *J Electroceram* 2007, **19**: 251-257.

[57] Takenaka T, Nagata H, Hiruma Y, *et al.* Lead-free piezoelectric ceramics based on perovskite structures. *J Electroceram* 2007, **19**: 259-265.

[58] Rödel J, Jo W, Seifert KTP, *et al.* Perspective on the development of lead-free piezoceramics. *J Am Ceram Soc* 2009, **92**: 1153-1177.

[59] Panda PK. Review: Environmental friendly lead-free piezoelectric materials. *J Mater Sci* 2009, **44**: 5049-5062.

[60] Safari A, Abazari M. Lead-free piezoelectric ceramics and thin films. *IEEE Trans Ultrason Ferroelectr Freq Control* 2010, **57**: 2165-2176.

[61] Tennery VJ, Hang KW. Thermal and X-ray diffraction studies of $NaNbO_3$-NbO_3 system. *J Appl Phys* 1968, **39**: 4749-4753.

[62] Ahtee M, Hewat AW. Structural phase-transitions in sodium-potassium niobate solid-solutions by neutron powder diffraction. *Acta Crystallogr A* 1978, **34**: 309-317.

[63] Egerton L, Dillon DM. Piezoelectric and dielectric properties of ceramics in the system potassium sodium niobate. *J Am Ceram Soc* 1959, **42**: 438-442.

[64] Dai YJ, Zhang XW, Chen KP. Morphotropic phase boundary and electrical properties of $K_{1-x}Na_xNbO_3$ lead-free ceramics. *Appl Phys Lett* 2009, **94**: 042905.

[65] Zhou JJ, Li JF, Wang K, *et al.* Phase structure and electrical properties of (Li,Ta)-doped (K,Na)NbO_3 lead-free piezoceramics in the vicinity of Na/K = 50/50. *J Mater Sci* 2011, **46**: 5111-5116.

[66] Trodahl HJ, Klein N, Damjanovic D, *et al.* Raman spectroscopy of (K,Na)NbO_3 and $(K,Na)_{1-x}Li_xNbO_3$. *Appl Phys Lett* 2008, **93**: 3.

[67] Wang K, Li JF. Analysis of crystallographic evolution in (Na,K)NbO_3-based lead-free piezoceramics by X-ray diffraction. *Appl Phys Lett* 2007, **91**: 262902.

[68] Ahtee M, Glazer AM. Lattice-parameters and tilted octahedra in sodium-potassium niobate solid-solutions. *Acta Crystallogr A* 1976, **32**: 434-446.

[69] Shirane G, Newnham R, Pepinsky R. Dielectric properties and phase transitions of $NaNbO_3$ and (Na,K)NbO_3. *Physical Review* 1954, **96**: 581-588.

[70] Hewat AW. Cubic-tetragonal-orthorhombic-rhombohedral ferroelectric transitions in perovskite potassium niobate - neutron powder profile refine ment of structures. *J Phys C: Solid State Phys* 1973, **6**: 2559-2572.

[71] Kakimoto K, Akao K, Guo YP, *et al.* Raman scattering study of piezoelectric $(Na_{0.5}K_{0.5})NbO_3$-$LiNbO_3$ ceramics. *Jpn J Appl Phys* 2005, **44**: 7064-7067.

[72] Kano J, Sasanuma K, Tsukada S, *et al.* Piezoelectric $(Na_{0.5}K_{0.5})NbO_3$-$SrTiO_3$ ceramics in the tetragonal-orthorhombic phase boundary studied by Raman spectroscopy. *Ferroelectrics* 2007, **347**: 55-59.

[73] Zhou JJ, Li JF, Zhang XW. Orthorhombic to tetragonal phase transition due to stress release in (Li,Ta)-doped (K,Na)NbO_3 lead-free piezoceramics. *J Eur Ceram Soc* 2012, **32**: 267-270.

[74] Liu W, Ren X. Large piezoelectric effect in Pb-free ceramics. *Phys Rev Lett* 2009, **103**: 257602.

[75] Xue D, Zhou Y, Bao H, *et al.* Large piezoelectric effect in Pb-free Ba(Ti,Sn)O_3-x(Ba,Ca)TiO_3 ceramics. *Appl Phys Lett* 2011, **99**: 122901.

[76] Jaeger RE, Egerton L. Hot pressing of potassium-sodium niobates. *J Am Ceram Soc* 1962, **45**: 209-213.

[77] Haertling GH. Properties of hot-pressed ferroelectric alkali niobate ceramics. *J Am Ceram Soc* 1967, **50**: 329-330.

[78] Li JF, Wang K, Zhang BP, *et al.* Ferroelectric and piezoelectric properties of fine-grained $Na_{0.5}K_{0.5}NbO_3$ lead-free piezoelectric ceramics prepared by spark plasma sintering. *J Am Ceram Soc* 2006, **89**: 706-709.

[79] Zhang BP, Li JF, Wang K, *et al.* Compositional dependence of piezoelectric properties in $Na_xK_{1-x}NbO_3$ lerad-free ceramics prepared by spark plasma sintering. *J Am Ceram Soc* 2006, **89**: 1605-1609.

[80] Wang K, Zhang BP, Li JF, *et al.* Lead-free $Na_{0.5}K_{0.5}NbO_3$ piezoelectric ceramics fabricated by spark plasma sintering: Annealing effect on electrical properties. *J Electroceram* 2008, **21**: 251-254.

[81] Shen ZY, Li JF, Wang K, Electrical and mechanical properties of fine-grained Li/Ta-modified (Na,K)NbO_3-based piezoceramics prepared by spark plasma sintering. *J Am Ceram Soc* 2010, **93**: 1378-1383.

[82] Liu N, Wang K, Li JF, *et al.* Hydrothermal synthesis and spark plasma sintering of (K,Na)NbO_3 lead-free piezoceramics. *J Am Ceram Soc* 2009, **92**: 1884-1887.

[83] Zhen Y, Li JF, Wang K, *et al.* Spark plasma sintering of Li/Ta-modified (K,Na)NbO_3 lead-free piezoelectric ceramics: Post-annealing temperature effect on phase structure, electrical properties and grain growth behavior. *Mater Sci Eng B-Adv Funct Solid-State Mater* 2011, **176**: 1110-1114.

[84] Arlt G, Hennings D, Dewith G. Dielectric-properties of fine-grained barium-titanate ceramics. *J Appl Phys* 1985, **58**: 1619-1625.

[85] Zhen YH, Li JF. Normal sintering of (K,Na)NbO_3-based ceramics: influence of sintering temperature on densification, microstructure, and electrical properties. *J Am Ceram Soc* 2006, **89**: 3669-3675.

[86] Li JF, Zhen YH, Zhang BP, *et al.* Normal sintering of (K,Na)NbO_3-based lead-free piezoelectric ceramics. *Ceram Int* 2008, **34**: 783-786.

[87] Shen ZY, Zhen YH, Wang K, *et al.* Influence of sintering temperature on grain growth and phase structure of compositionally optimized high-performance Li/Ta-modified (Na,K)NbO_3 ceramics. *J Am Ceram Soc* 2009, **92**: 1748-1752.

[88] Shen ZY, Wang K, Li JF. Combined effects of Li content and sintering temperature on polymorphic phase boundary and electrical properties of Li/Ta Co-doped (Na, K)NbO_3 lead-free piezoceramics. *Appl Phys A* 2009, **97**: 911-917.

[89] Zhen YH, Li JF. Abnormal grain growth and new core-shell structure in (K,Na)NbO_3-based lead-free piezoelectric ceramics. *J Am Ceram Soc* 2007, **90**: 3496-3502.

[90] Wang K, Li JF. Low-temperature sintering of Li-modified (K,Na)NbO_3 lead-free ceramics: Sintering behavior, microstructure, and electrical properties. *J Am Ceram Soc* 2010, **93**: 1101-1107.

[91] Kingery WD. Densification during sintering in the presence of a liquid phase. I. theory. *J Appl Phys* 1959, **30**: 301-306.

[92] Yoo J, Lee K, Chung K, *et al.* Piezoelectric and dielectric properties of (LiNaK)(NbTaSb)O_3 ceramics with variation in poling temperature. *Jpn J Appl Phys* 2006, **45**: 7444-7448.

[93] Du HL, Tang FS, Luo F, *et al.* Effect of poling condition on piezoelectric properties of ($K_{0.5}Na_{0.5}$) NbO_3-$LiNbO_3$ lead-free piezoelectric ceramics. *Mater Sci Eng B-Solid State Mater Adv Technol* 2007, **137**: 175-179.

[94] Du HL, Zhou WC, Luo F, *et al.* An approach to further improve piezoelectric properties of ($K_{0.5}Na_{0.5}$)NbO_3-based lead-free ceramics. *Appl Phys Lett* 2007, **91**: 202907.

[95] Ogawa T, Furukawa M, Tsukada T. Poling field dependence of piezoelectric properties and hysteresis loops of polarization versus electric field in alkali niobate ceramics. *Jpn J Appl Phys* 2009, **48**.

[96] Rubio-Marcos F, Romero JJ, Ochoa DA, *et al.* Effects of poling process on KNN-modified piezo-ceramic properties. *J Am Ceram Soc* 2010, **93**: 318-321.

[97] Morozov MI, Kungl H, Hoffmann MJ. Effects of poling over the orthorhombic-tetragonal phase transition temperature in compositionally homogeneous (K,Na)NbO_3-based ceramics. *Appl Phys Lett* 2011, **98**.

[98] Zuo RZ, Fu J, Lv DY. Phase transformation and tunable piezoelectric properties of lead-free ($Na_{0.52}K_{0.48-x}li_x$)($Nb_{1-x-y}Sb_yTa_x$)O_3 system. *J Am Ceram Soc* 2009, **92**: 283-285.

[99] Gao Y, Zhang J, Qing Y, *et al.* Remarkably strong piezoelectricity of lead-free ($K_{0.45}Na_{0.55}$)$_{0.98}Li_{0.02}$($Nb_{0.77}Ta_{0.18}Sb_{0.05}$)$O_3$ ceramic. *J Am Ceram Soc* 2011, **94**: 2968-2973.

[100] Safari A, Akdogan EK. Piezoelectric and Acoustic Materials for Transducer Applications. New York: Springer, 2008.

[101] Zhen YH, Li JF, Wang K. Fabrication and electrical properties of fine-scale 1-3 piezoceramic/ epoxy composites using (K,Na)NbO_3-based lead-free ceramics. *Ferroelectrics* 2007, **358**: 1043-1050.

[102] Shen ZY, Xu Y, Li JF. Fabrication and electromechanical properties of microscale 1-3-type piezoelectric composites using (Na,K)NbO_3-based Pb-free piezoceramics. *J Appl Phys* 2009, **105**.

[103] Shen ZY, Li JF, Chen R, *et al.* Microscale 1-3-type (Na,K)NbO_3-based Pb-free piezocomposites for high-frequency ultrasonic transducer applications. *J Am Ceram Soc* 2011, **94**: 1346-1349.

[104] Shung KK, Cannata JM, Zhou QF. Piezoelectric materials for high frequency medical imaging applications: a review. *J Electroceram* 2007, **19**: 139-145.

[105] Guo M, Lam KH, Lin DM, *et al.* A rosen-type piezoelectric transformer employing lead-free $K_{0.5}Na_{0.5}NbO_3$ ceramics. *J Mater Sci* 2008, **43**: 709-714.

[106] Hagh NM, Jadidian B, Ashbahian E, *et al.* Lead-free piezoelectric ceramic transducer in the donor-doped $K_{1/2}Na_{1/2}NbO_3$ solid solution system. *IEEE Trans Ultrason Ferroelectr Freq Control* 2008, **55**: 214-224.

[107] Kwok KW, Hon SF, Lin D. Lead-free self-focused piezoelectric transducers for viscous liquid ejection. *Sensor Actuat a-Phys* 2011, **168**: 168-171.